

Ophidiomyces ophiodiicola, Etiologic Agent of Snake Fungal Disease, in Europe since Late 1950s

Francesco C. Origgi, Simone R.R. Pisano, Olivier Glairot, Stefan T. Hertwig, Andreas Schmitz, Sylvain Ursenbacher

The fungus *Ophidiomyces ophiodiicola* is the etiologic agent of snake fungal disease. Recent findings date US occurrence at least as far back as 1945. We analyzed 22 free-ranging snakes with gross lesions consistent with snake fungal disease from museum collections from Europe. We found 5 positive samples, the oldest collected in 1959.

In the past few decades, fungal agents have surfaced as relevant threats to conservation and biodiversity among both ectotherms and endotherms (1–3). The emerging fungal agent *Ophidiomyces ophiodiicola* has been detected in both captive and free-ranging snakes in the United States in the past 16 years (4–7) and more recently in the United Kingdom and Czech Republic (8). *O. ophiodiicola* fungus has been associated with a variably severe dermatitis but also multisystemic disease (9). Experimental infections (10) demonstrated the causative association between *O. ophiodiicola* infection and snake fungal disease (SFD), the common name attributed to the disease caused by this fungus. The effect on free-ranging populations of snakes is not completely understood, but many species of snakes appear to be susceptible and different populations appear to have been negatively affected (9,11).

A recent article showed that the earliest evidence of *O. ophiodiicola* infection in North America dates

back to 1945 (12). However, records of *O. ophiodiicola* fungi in Europe date back only to 2010–2016 (8). Detection of 2 phylogenetically distinct lineages in the United States and Europe consistent with genetic differences between the clades, presumably reflects independent evolution of the lineages. To acquire additional data about the origins of this agent in Europe, we obtained skin samples from free-ranging snake collections from multiple natural history museums in Switzerland.

The Study

We selected 22 skin samples with macroscopic lesions consistent with SFD out of 1,100 free ranging snakes examined from the collections of 3 natural history museums in Switzerland (Table 1; Appendix, <https://wwwnc.cdc.gov/EID/article/28/10/22-0564-App1.pdf>). We collected tissue samples from the integument of snakes showing obvious macroscopic lesions consistent with dermatitis (Appendix Figure 1). Snake specimens were preserved in 100% ethanol. We collected tissue samples using sterile instrumentation changed between each sampling. We placed each tissue sample in a cryotube containing an aliquot of absolute ethanol. Upon delivery at the laboratory, tissue samples were split into 2 portions for processing for DNA extraction and histopathology (Appendix).

We performed PCR according to various protocols aiming to detect multiple gene targets belonging to the *O. ophiodiicola* genome. Initial screening for the presence of *O. ophiodiicola* fungi was performed by applying a modified PCR protocol (an original protocol performed in a conventional PCR setting) (13) targeting the partial sequence of the intergenic spacer (IGS). We then tested positive samples and, later, negative samples to rule out false-negative results

Author affiliations: University of Bern, Bern, Switzerland (F.C. Origgi, S.R.R. Pisano, S.T. Hertwig); Museum of Zoology, Lausanne, Switzerland (O. Glairot); University of Lausanne, Lausanne (O. Glairot); Naturhistorisches Museum Burgergemeinde Bern, Bern (S.T. Hertwig); Natural History Museum of Geneva, Geneva, Switzerland (A. Schmitz); University of Basel, Basel, Switzerland (S. Ursenbacher); info fauna CSCF & karch, Neuchâtel, Switzerland (S. Ursenbacher).

DOI: <https://doi.org/10.3201/eid2810.220564>

Table 1. Museum tissue samples from snakes of genera *Natrix* and *Vipera* used in investigation of snake fungal disease in Europe*

Sample	Museum	Species	ID	Sex	Year	Location (country)
1	NMBE	<i>Natrix helvetica</i>	1049780	F	2001	Erlach (Switzerland)
2†	NMBE	<i>N. helvetica</i>	1056184	NA	2007	Tavannes (Switzerland)
3‡	NMBE	<i>Vipera aspis</i>	1072979	NA	2015	Grandvillars (Switzerland)
4	MHNG	<i>N. tessellata</i>	1402.040	F	1972	Lake Geneva (Switzerland)
5‡	MHNG	<i>N. natrix</i>	851.077	NA	NA	NS (Czech Republic)
6	MHNG	<i>N. natrix</i>	1342.87	NA	1963	Thurgau (Switzerland)
7	MHNG	<i>N. helvetica</i>	1137.18	NA	1967	NS (Italy)
8†	MHNG	<i>N. tessellata</i>	1386.55	F	1969	Tessin (Switzerland)
9	MHNG	<i>N. helvetica</i>	1397.21	NA	1959	NS (Italy)
10	MHNG	<i>N. helvetica</i>	2430.91	NA	1986	Zurich (Switzerland)
11†	MHNG	<i>N. maura</i>	1199.084	F	1971	Haute-Savoie (France)
12	MHNG	<i>N. tessellata</i>	1387.60	F	1961	Maggia (Switzerland)
13	MZL	<i>N. tessellata</i>	MZL41123	F	2008	Lake Geneva (Switzerland)
14†	MZL	<i>N. tessellata</i>	MZL30407	F	2007	Lake Geneva (Switzerland)
15‡	MZL	<i>N. tessellata</i>	MZL41142	M	2009	Lake Geneva (Switzerland)
16	MZL	<i>N. tessellata</i>	MZL30508	F	2007	Lake Geneva (Switzerland)
17‡	MZL	<i>N. tessellata</i>	MZL40905	F	2012	Lake Geneva (Switzerland)
18	MZL	<i>N. tessellata</i>	MZL31837	F	2010	Lake Geneva (Switzerland)
19	MZL	<i>N. tessellata</i>	MZL30505	NA	2007	Lake Geneva (Switzerland)
20	MZL	<i>N. tessellata</i>	MZL41144	F	2009	Lake Geneva (Switzerland)
21†	MZL	<i>N. tessellata</i>	MZL40911	F	2013	Lake Geneva (Switzerland)
22	MZL	<i>N. tessellata</i>	MZL31839	M	2010	Lake Geneva (Switzerland)

*Bold indicated PCR-positive samples with presence of fungal hyphae. MZL, Museum of Zoology, Lausanne; NMBE, Natural History Museum of Bern; MHNG, Natural History Museum of Geneva; NA, not available; NS, not specified.

†PCR-negative samples with presence of fungal hyphae and with histological lesions similar to those observed in the PCR-positive samples.

‡PCR-negative samples with presence of fungal hyphae and with histological lesions dissimilar to those observed in the PCR-positive samples.

by IGS PCR by using 3 additional newly developed protocols targeting distinct genome sequences: the 5.8–28s RNA internal transcribed spacer (ITS) 2, the transcription elongation factor (TEF), and the actin genes (Appendix). We used nucleotide sequences obtained from each of the readable PCR amplicons for phylogenetic analysis. We used partial sequences from the amplified ITS, TEF, and actin targets to build up a maximum-likelihood phylogenetic tree for each of the amplified genomic sequences (Appendix). All 22 samples examined for the presence of *O. ophioidicola* genomic DNA were characterized by gross and microscopic lesions consistent with dermatitis (Table 2; Appendix Figures 1–3).

Overall, we observed fungal elements in 14/22 examined tissue sections. All samples positive for SFD by PCR were characterized by the presence of intralesional fungal hyphae and heterophilic granulomas or microabscesses (Appendix Figures 2, 3); we observed intradermal granulomas in 1 sample, in which we could not histologically detect any fungal elements. When we used the original IGS-PCR protocol (13), 5/22 samples yielded a detectable band (sample numbers 1, 6, 7, 9, and 12). Samples 6, 7, 9, and 12 were also confirmed positive when we used the ITS primer set. Four of 22 samples (6, 7, 9, and 12) yielded a detectable band when we used the actin primer set. Two of 22 samples (9 and 12) yielded a detectable band when we used the TEF primer set. Despite positive IGS amplification, we could not

amplify sample 1 with either the actin or the TEF primer sets. We obtained a nonspecific amplification with the ITS primer set and consequently did not further consider sample 1 for sequence comparison and phylogenetic analysis (Appendix, Figure 4).

Sequence alignments, reflected in the phylogenetic trees (Appendix Figure 4), showed unique single-nucleotide polymorphisms clearly separating the museum samples from Switzerland into either the clade circulating in Europe or the one circulating in North America (Figure) (8). Results were consistent across the partial sequences of the targeted ITS, TEF, and actin genomic regions. Specifically, samples 7 and 9 from Italy always clustered within the clade from Europe, whereas 6 and 12 from Switzerland clustered within the clade from North America (Appendix Figure 4).

Conclusions

Our research, conducted similarly to an investigation performed in North America, provided evidence of the presence of *O. ophioidicola* infection in free-ranging snakes in Europe at least since 1959 (12). Our findings were supported by test results for 4 distinct molecular targets and consistent histological findings. Furthermore, all PCR-positive samples confirmed by sequencing were also associated with the presence of intralesional fungal structures consistent with *O. ophioidicola* and associated with an obvious inflammatory reaction.

Of note, supporting data are consistent with the surprising finding that the proposed clades from both North America and Europe (8) have been present at least since the early 1960s. Furthermore, because our dataset spanned only 1959–2012, *O. ophioidiicola* fungi might have been present in Europe even before 1959. The significance of both clades existing in Europe will require further investigations. In spite of the absence in the United States of any strain proven to belong to the clade from Europe, introduction cannot be completely ruled out (14). In an alternative scenario, the clade from North America might have been introduced into Europe before the 1950s. At the moment, the colonization of *O. ophioidiicola* fungi on the European continent appears to have occurred several decades before proposed (8).

Detection of *O. ophioidiicola* fungi in Italy and Switzerland north of the Alps, further expands

its known distribution in Europe. Curiously, Switzerland appears to be the only country in Europe where the clade of *O. ophioidiicola* fungi from North America has to date been identified. However, sampling bias secondary to the restricted sampling area selected cannot be ruled out. Finally, although the 2 samples from Switzerland that clustered with the clade from North America were from different regions, the regions are located relatively close geographically to one another (160 km or ≈100 miles).

In summary, this investigation supports the presence of *O. ophioidiicola* fungi in Europe since at least 1959 with genomic sequences compatible with the 2 known lineages. These results provide critical elements for helping to rethink disease ecology and global distribution of *O. ophioidiicola* fungi and reconstructing its natural history.

Table 2. Histologic findings from investigation of snake fungal disease in Europe*

Sample	Light microscopy descriptions	PAS findings	Score†
1	Epidermal hyperplasia with serocellular crusts and histiocytic granulomas; mononuclear to heterophilic dermatitis	Septate fungal hyphae, 3 μm thick, branching both at 90 and 45 degrees	3
2	Epidermal hyperplasia with serocellular crusts and microabscesses	Rare, septate fungal hyphae, 2–3 μm thick, branching at 90 degrees	2
3	Epidermal ulceration with heterophilic infiltration and histiocytic dermatitis, intralesional bacteria and foreign material	Septate fungal hyphae, 3 μm thick, branching at 90 degrees	1
4	Ulcerative dermatitis with serocellular crusts and hyperkeratosis	No evidence of fungal hyphae	0
5	Hyperkeratosis	Septate fungal hyphae, embedded in the keratin, 2–3 μm thick, branching at 90 degrees and acute angle	1
6	Hyperkeratosis with histiocytic (granulomatous) dermatitis	Septate fungal hyphae, 3–4 μm thick, branching at acute angle	3
7	Heterophilic granulomas and microabscesses in the epidermis	Rare fungal hyphae, 3 μm thick embedded or associated with the microgranulomas	3
8	Hyperkeratosis with serocellular crusts, epidermal microgranulomas and lymphocytic dermatitis	Septate fungal hyphae, 3 μm thick, branching at 90 degrees and acute angle	2
9	Large crusts surrounded by histiocytic to heterophilic infiltrate and multifocal microgranulomas	Fungal hyphae in the crusts, 2–3 μm thick	3
10	Few crust fragments admixed with bacteria	No detectable fungal hyphae	0
11	Lympho-histiocytic dermatitis with dermal heterophilic granulomas	Rare fragmented hyphae in the heterophilic granulomas	2
12	Serocellular crusts together with large heterophilic granulomas and more diffused histiocytic infiltration; lympho-histiocytic dermatitis	Septate fungal hyphae, 3 μm thick, branching at 90 degrees or acute angle	3
13	Small serocellular crusts	No evidence of fungal hyphae	0
14	Small and rare heterophilic granulomas	Fragments of fungal hyphae in microgranulomas	2
15	A small serocellular crust	Few fungal septate hyphae, 2–3 μm thick, branching at 90 degrees	1
16	Severe dermal edema with isolated inflammatory cells	No obvious fungal elements	0
17	Serocellular crusts with intralesional bacteria	Fragments of non-septate hyphae	1
18	Hyperkeratosis with upper keratin heterophilic to histiocytic infiltration	No obvious fungal elements	0
19	Serocellular crust	No obvious fungal elements	0
20	Intralesional heterophilic granulomas	No obvious fungal elements	0
21	Epidermal heterophilic granulomas with serocellular crusts	Septate fungal hyphae, 2–3 μm thick, branching at 90 degrees	2
22	Intraepidermal crusts with heterophilic granulomas and intralesional bacteria	No obvious fungal elements	0

*PAS, periodic acid–Schiff.

†Subjective scoring system complementing morphologic and molecular data; 0, PCR-negative with no histologic evidence of fungi; 1, PCR-negative with presence of fungi but without lesions consistent with those observed in PCR-positive samples (absence of heterophilic granulomas); 2, PCR-negative with presence of fungi and lesions consistent with snake fungal disease; 3, PCR-positive with presence of fungi consistent with *Ophiomyces ophioidiicola*.

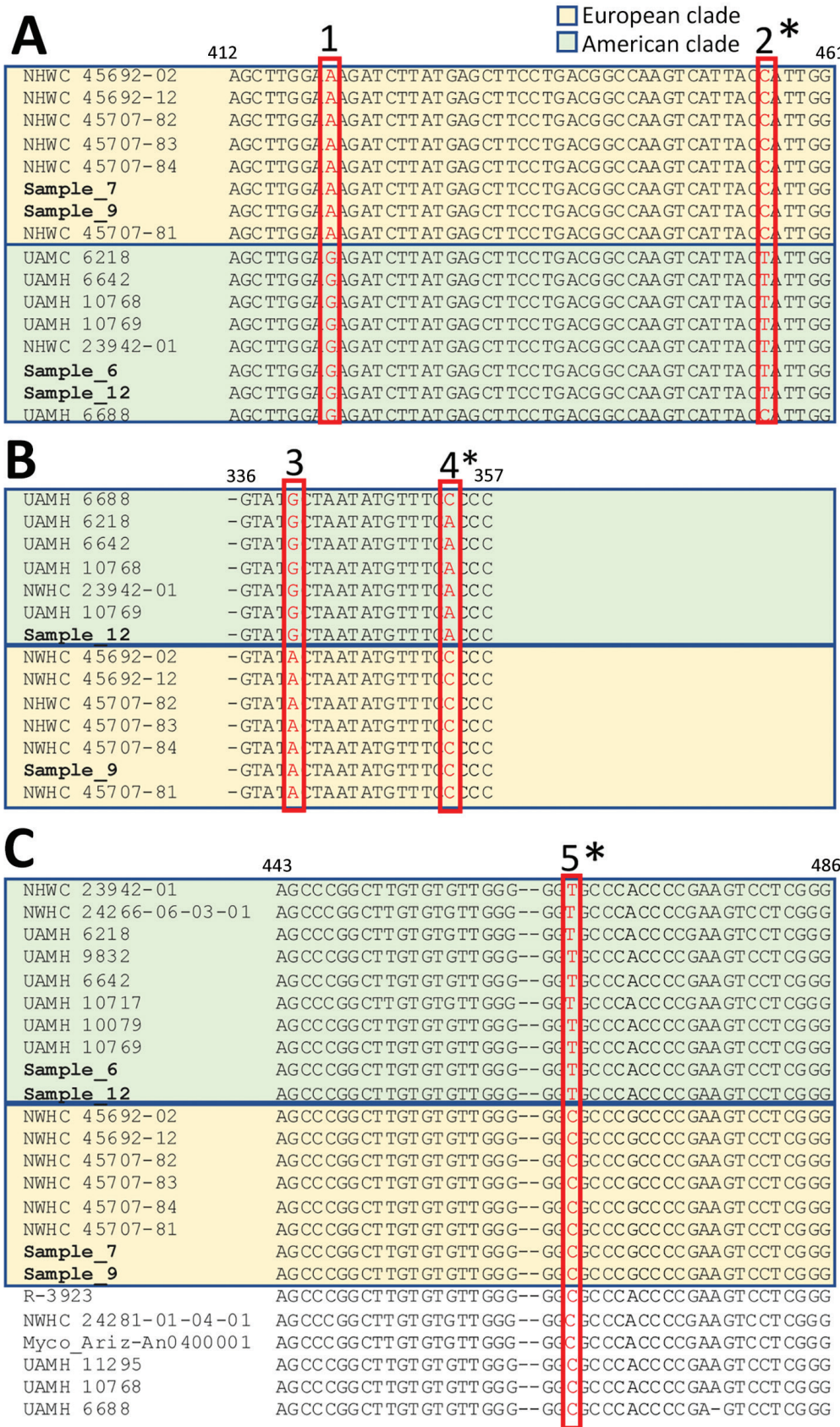


Figure. Nucleotide sequence alignment of selected sections of *Ophidiomyces ophiodiicola* from free-ranging snake collections from multiple natural history museums in Switzerland (bold) compared with reference sequences. Amplicons obtained with different PCR primer sets highlight single-nucleotide polymorphisms (SNPs, red boxes) unique to either the European (pastel gold) or American (pastel green) clades. PCR primer results: A) actin; B) transcription elongation factor; and C) internal transcribed spacer. The isolate UAMH 6688 (UK strain) shares 2/5 unique SNPs with the members of the clade from North America, whereas 3 of them (single asterisks) are shared with strains from Europe. These differences match the divergent branching of this strain in the clades from both North America and Europe. Similarly, 5 others fungal isolates (double asterisks)—R-3923; NWHC 24281-01-04-01, Myco_Ariz-An040001, UAMH 11295, and UAMH 10768, in addition to UAMH 6688, originating from the United States, Australia, and the United Kingdom—shared the internal transcribed spacer SNP of the clade from Europe and clustered consistently in an intermediate group in the corresponding phylogenetic tree (Appendix Figure 4, <https://wwwnc.cdc.gov/EID/article/28/10/22-0564-App1.pdf>).

Acknowledgments

We thank the Natural History Museum of Bern, the Natural History Museum of Geneva, the Museum of Zoology of Lausanne, and David Guerra for help during the sampling.

This work was partially financed by the Swiss Federal Office for the Environment (grant no. 05.0040.PZ/R413-2016).

About the Author

Dr. Origgi is a veterinary microbiologist and pathologist with strong interest in infectious diseases and associated pathogenesis in wildlife and nondomestic animals.

References

- Hoyt JR, Kilpatrick AM, Langwig KE. Ecology and impacts of white-nose syndrome on bats. *Nat Rev Microbiol*. 2021;19:196–210. <https://doi.org/10.1038/s41579-020-00493-5>
- Martel A, Spitzen-van der Sluijs A, Blooi M, Bert W, Ducatelle R, Fisher MC, et al. *Batrachochytrium salamandrivorans* sp. nov. causes lethal chytridiomycosis in amphibians. *Proc Natl Acad Sci U S A*. 2013;110:15325–9. <https://doi.org/10.1073/pnas.1307356110>
- O'Hanlon SJ, Rieux A, Farrer RA, Rosa GM, Waldman B, Bataille A, et al. Recent Asian origin of chytrid fungi causing global amphibian declines. *Science*. 2018;360:621–7. <https://doi.org/10.1126/science.aar1965>
- Clark RW, Marchand MN, Clifford BJ, Stechert R, Stephens S. Decline of an isolated timber rattlesnake (*Crotalus horridus*) population: interactions between climate change, disease, and loss of genetic diversity. *Biol Conserv*. 2011;144:886–91. <https://doi.org/10.1016/j.biocon.2010.12.001>
- Allender MC, Dreslik M, Wylie S, Phillips C, Wylie DB, Maddox C, et al. *Chryso sporium* sp. infection in eastern massasauga rattlesnakes. *Emerg Infect Dis*. 2011;17:2383–4. <https://doi.org/10.3201/eid1712.110240>
- Sigler L, Hambleton S, Paré JA. Molecular characterization of reptile pathogens currently known as members of the *Chryso sporium* anamorph of *Nannizziopsis vriesii* complex and relationship with some human-associated isolates. *J Clin Microbiol*. 2013;51:3338–57. <https://doi.org/10.1128/JCM.01465-13>
- McKenzie CM, Oesterle PT, Stevens B, Shirose L, Lillie BN, Davy CM, et al. Pathology associated with ophidiomycosis in wild snakes in Ontario, Canada. *Can Vet J*. 2020;61:957–62.
- Franklinos LHV, Lorch JM, Bohuski E, Rodriguez-Ramos Fernandez J, Wright ON, Fitzpatrick L, et al. Emerging fungal pathogen *Ophidiomyces ophiodiicola* in wild European snakes. *Sci Rep*. 2017;7:3844. <https://doi.org/10.1038/s41598-017-03352-1>
- Lorch JM, Knowles S, Lankton JS, Michell K, Edwards JL, Kapfer JM, et al. Snake fungal disease: an emerging threat to wild snakes. *Philos Trans R Soc Lond B Biol Sci*. 2016;371:20150457.
- Lorch JM, Lankton J, Werner K, Falendysz EA, McCurley K, Bleher DS. Experimental infection of snakes with *Ophidiomyces ophiodiicola* causes pathological changes that typify snake fungal disease. *mBio*. 2015;6:e01534–15. <https://doi.org/10.1128/mBio.01534-15>
- Davy CM, Shirose L, Campbell D, Dillon R, McKenzie C, Nemeth N, et al. Revisiting Ophidiomycosis (snake fungal disease) after a decade of targeted research. *Front Vet Sci*. 2021;8:665805. <https://doi.org/10.3389/fvets.2021.665805>
- Lorch JM, Price SJ, Lankton JS, Drayer AN. Confirmed cases of ophidiomycosis in museum specimens from as early as 1945, United States. *Emerg Infect Dis*. 2021;27:1986–9. <https://doi.org/10.3201/eid2707.204864>
- Bohuski E, Lorch JM, Griffin KM, Bleher DS. TaqMan real-time polymerase chain reaction for detection of *Ophidiomyces ophiodiicola*, the fungus associated with snake fungal disease. *BMC Vet Res*. 2015;11:95. <https://doi.org/10.1186/s12917-015-0407-8>
- Ladner JT, Palmer JM, Ettinger CL, Stajich JE, Farrell TM, Glorioso BM, et al. The population genetics of the causative agent of snake fungal disease indicate recent introductions to the USA. *PLoS Biol*. 2022;20:e3001676. <https://doi.org/10.1371/journal.pbio.3001676>

Address for correspondence: Francesco C. Origgi, Institute of Animal Pathology (ITPA), Vetsuisse Faculty, University of Bern, Länggassstrasse 122, CH-3012, Bern, Switzerland; email: francesco.origgi@vetsuisse.unibe.ch

Ophiodiomyces ophiodiicola, Etiologic Agent of Snake Fungal Disease, in Europe since Late 1950s

Appendix

Additional Methodology

Sample Selection

We assessed 1,100 individual snakes, mainly *Natrix* spp., *Hierophis viridiflavus*, and a few vipers (*V. berus*). Most ($\approx 95\%$) were from Switzerland; the remaining snakes were from the surrounding countries, mainly Germany and Italy, and a few from France and Czech Republic. While they were still in preservation jars, we visually assessed these snake specimens by examining the dorsal and ventral scales; when putative dermatitis was observed (macroscopic darkening of the scales with pitting, fragmentation, lifting, and detachment), we removed the snakes from the jars and observed them more closely. If a lesion was confirmed on closer inspection, then we sampled the snake. We included only adult and subadult snakes in this study.

Tissue Processing for DNA Extraction and Histological Slide Preparation

DNA extraction was performed using the Qiagen DNeasy extraction kit (<https://www.qiagen.com>) according to the manufacturer's instruction. DNA amount and purity was assessed using the ThermoFisher Nanodrop spectrophotometer (<https://www.thermofisher.com>) and stored at 4°C prior downstream analysis. Histopathology was performed following the current protocols used at the Institute of Animal Pathology (ITPA) of the University of Bern. Briefly, the tissues were first dehydrated and then embedded in paraffin blocks, which were then sectioned 5 μm thick and stained with hematoxylin and eosin. Periodic acid Schiff (PAS), a special stain commonly used to detect fungal organisms in tissues, was applied to each of the examined sections.

Molecular Investigation

Given that the tissues samples from the museums had been fixed for up to several decades and DNA fragmentation might have occurred, we designed specific primers

amplifying DNA fragments no longer than 200bp. More specifically a forward (5'-TGTCGAGCGTCATTGCAACC-3') and reverse (5'-AACAGATTCCCATACACTCAGACACC-3') primer amplifying the partial sequence of the ITS, a forward (5'-CCAGCCCAACTATCAAACCTTTGGC-3') and a reverse (5'-TGATACCACGCTCAGCTCGG-3') primer amplifying the partial sequence of the TEF gene, and a forward (5'-TTAGATTTCCAGCAAGAGATCCAGACTG-3') and a reverse (5'-CCAAGACGCTGGGTTGGAAAAG-3') primer amplifying the partial sequence of the ACT gene were designed. The primer sets were selected attempting to target the most polymorphic regions across the selected sequences. DNA amplification was carried similarly for all the different targets. More specifically, 1 µL of 100 µM suspension of the selected forward and reverse primer were added to a mix including 3.75 µL of a 25 mM MgCl₂ solution, 3 µL of 10X buffer, 0.4 µL of a 10 mM dNTPs mix, 0.2 µL Firepol DNA polymerase (Solis BioDyne-Lucerna-chem, CH), 100 ng of DNA target, and ddH₂O up to 30 µL. Cycling included a denaturing step at 94°C for 3 minutes followed by 40 cycles comprising a 30 second long 94°C denaturing step, an annealing step at 52°C for 30 seconds and an extension step at 72°C for 30 seconds. A 10 minutes long final extension step at 72°C followed. The samples were then resolved in a 2% agarose gel and examined under UV lights.

Phylogenic Analysis

The phylogenetic trees were built by comparing the sequences obtained from the investigated samples in this study together with a set of homologous sequences available in GenBank comprising strains belonging either to the European or the North American lineage of *O. ophioidicola* together with an unrelated fungus serving as outgroup (*Pseudoamauroascus australiensis*) (ACT: KY474070.1 = NWHC 45692-02; KY474071.1 = NWHC 45692-12; KY474073.1 = NWHC 45707-82; KY474074.1 = NWHC 45707-83; KY474075.1 = NWHC 45707-84; KY474072.1 = NWHC 45707-81; KY474066.1 = UAMH 6218; KY474067.1 = UAMH 6642; KY474068.1 = UAMH 10768; KY474069.1 = UAMH 10769; KY474076.1 = NWHC 23942-01; KY474078.1 = UAMH 6688; UAMH8392 = *Pseudoamauroascus australiensis* outgroup; TEF: KY474092.1 = *Pseudoamauroascus australiensis* (UAMH 8392) outgroup; KY474082.1 = UAMH 6688; KY474080.1 = UAMH 6218; KY474081.1 = UAMH 6642; KY474083.1 = UAMH 10768; KY474091.1 = NWHC 23942-01; KY474084.1 = UAMH 10769; KY474085.1 = NWHC 45692-02; KY474086.1 = NWHC 45692-12; KY474088.1 = NWHC 45707-82; KY474089.1 = NWHC 45707-83; KY474090.1 = NWHC

45707–84; KY474087.1 = NWHC 45707–81; **ITS**: AJ131787.1 = *Pseudoamauroascus australiensis* outgroup; KY474065.1 = NWHC 23942–01; KX148657.1 = NWHC 24266–06–03–01; KF477227.1 = UAMH 6218; KF477229.1 = UAMH 9832; KC884267.1 = UAMH 6642; KF477233.1 = UAMH 10717; KF477231.1 = UAMH 10079; KF477235.1 = UAMH 10769; KY474059.1 = NWHC 45692–02; KY474060.1 = NWHC 45692–12; KY474062.1 = NWHC 45707–82; KY474063.1 = NWHC 45707–83; KY474064.1 = NWHC 45707–84; KY474061.1 = NWHC 45707–81; EU715819.1 = R-3923; KX148658.1 = NWHC 24281–01–04–01; KF225599.1 = MYCO-ARIZ AN0400001; KF477237.1 = UAMH 11295; KF477234.1 = UAMH 10768).

The nucleotide sequences were aligned using Muscle (<https://www.ebi.ac.uk/Tools/msa/muscle>) with standard settings and the resulting alignments were fed into Mega 7 (MEGA7: Molecular Evolutionary Genetics Analysis version 7.0 for bigger datasets. Kumar S, Stecher G, Tamura K. MEGA7: Molecular Evolutionary Genetics Analysis Version 7.0 for Bigger Datasets. Mol Biol Evol. 2016;33:1870–4.) to obtain a maximum likelihood phylogenetic tree. The substitution model used was the Tamura-Nei model with uniform rates among sites, complete deletion of gaps, 10,000 bootstrap replications. The alignments were 93 nt long for the ACT, 394 nt for the TEF, and 272 nt for the ITS trees.

Sequences

Here are listed all the sequences obtained during this investigation. For each sequence, length of the amplicon (with excised primers) and nucleotide mismatches are reported, shown bolded.

IGS (partial sequence of the intergenic spacer) 97 nt without primers

>Sample_1

TTACATTTTCCATACAAAAAGGTGG———G TCCGGCGACCC**CGGG**AAAAACCCTCG-
TTCCGCGGAAGACAAGCGCCCGGAGAGTAT

>Sample_6

TTACATTTTCCATACAAAAAGGTGGTCCCGACCCAGTCAGGTCCGGCGACCC**AGGG**AAAAACCCTCGGATCCGCGG
AAGACAAGCGCCCGGAGAGTAT

>Sample_7

TTACATTTTCCATACAAAAAGGTGGTCCCGACCCAGTCAGGTCCGGCGACCC**CGGG**AAAAACCCTCGGATCCGCGG
AAGACAAGCGCCCGGAGAGTAT

>Sample_9

TTACATTTTCCATACAAAAAGGTGGTCCCGACCCAGTCAGGTCCGGCGACCC**CGGG**AAAAACCCTCGGATCCGCGG
AAGACAAGCGCCCGGAGAGTAT

>Sample_12

TTACATTTTCCATACAAAAAGGTGGTCCCGACCCAGTCAGGTCCGGCGACCC**A**GGGAAAACCCTCGGATCCGCGG
AAGACAAGCGCCCGGAGAGTAT

ITS (5.8–28s RNA internal transcribed spacer 2) 100 nt without primers

>Sample_1 (non-specific amplification; not included in phylogenetic analysis)

___GTCCGAGTTGTCCGAGCGTCATTGCAACCCTGGACCATGCAGGTTGCTAAATGAGAAGAAGGTAgAGTCCCA
G___TGTNNTAGTGCTGTGGGGTGTCTGAGTGTATGGGAATCTGTTATCTG

>Sample_6

CCCTCAAGCCCGGCTTGTGTGTTGGGGG**T**GCCCACCCCGAAGTCCTCGGGCGCGGG**C**CCCCC**C**AAATGCAGTGG
CGGCACCGAGTTCCT

>Sample_7

CCCTCAAGCCCGGCTTGTGTGTTGGGGG**C**GCCCGCCCGAAGTCCTCGGGCGCGGG-
CCCCC**C**AAATGCAGTGGCGGCACCGAGTTCCT

>Sample_9

CCCTCAAGCCCGGCTTGTGTGTTGGGGG**C**GCCCGCCCGAAGTCCTCGGGCGCGGG-
CCCCC**C**AAATGCAGTGGCGGCACCGAGTTCCT

>Sample_12

CCCTCAAGCCCGGCTTGTGTGTTGGGGG**T**GCCCACCCCGAAGTCCTCGGGCGCGGG**C**CCCCC**C**AAATGCAGTGG
CGGCACCGAGTTCCT

ACT (actin gene) 92 nt without primers

>Sample_7

CTGCTCAGAGCTCTAGCTTGGAA**A**AGATCTTATGAGCTTCCTGACGGCCAAGTCATTACC**A**TTGGCAACGAGCGAT
TCCGTGCTCCCGAAGCC

>Sample_9

CTGCTCAGAGCTCTAGCTTGGAA**A**AGATCTTATGAGCTTCCTGACGGCCAAGTCATTACC**A**TTGGCAACGAGCGAT
TCCGTGCTCCCGAAGCC

>Sample_6

CTGCTCAGAGCTCTAGCTTGGAG**A**GATCTTATGAGCTTCCTGACGGCCAAGTCATTACT**A**TTGGCAACGAGCGAT
TCCGTGCTCCCGAAGCC

>Sample_12

CTGCTCAGAGCTCTAGCTTGGAG**A**GATCTTATGAGCTTCCTGACGGCCAAGTCATTACT**A**TTGGCAACGAGCGAT
TCCGTGCTCCCGAAGCC

TEF (transcription elongation factor) 158 nt without primers

>Sample_9

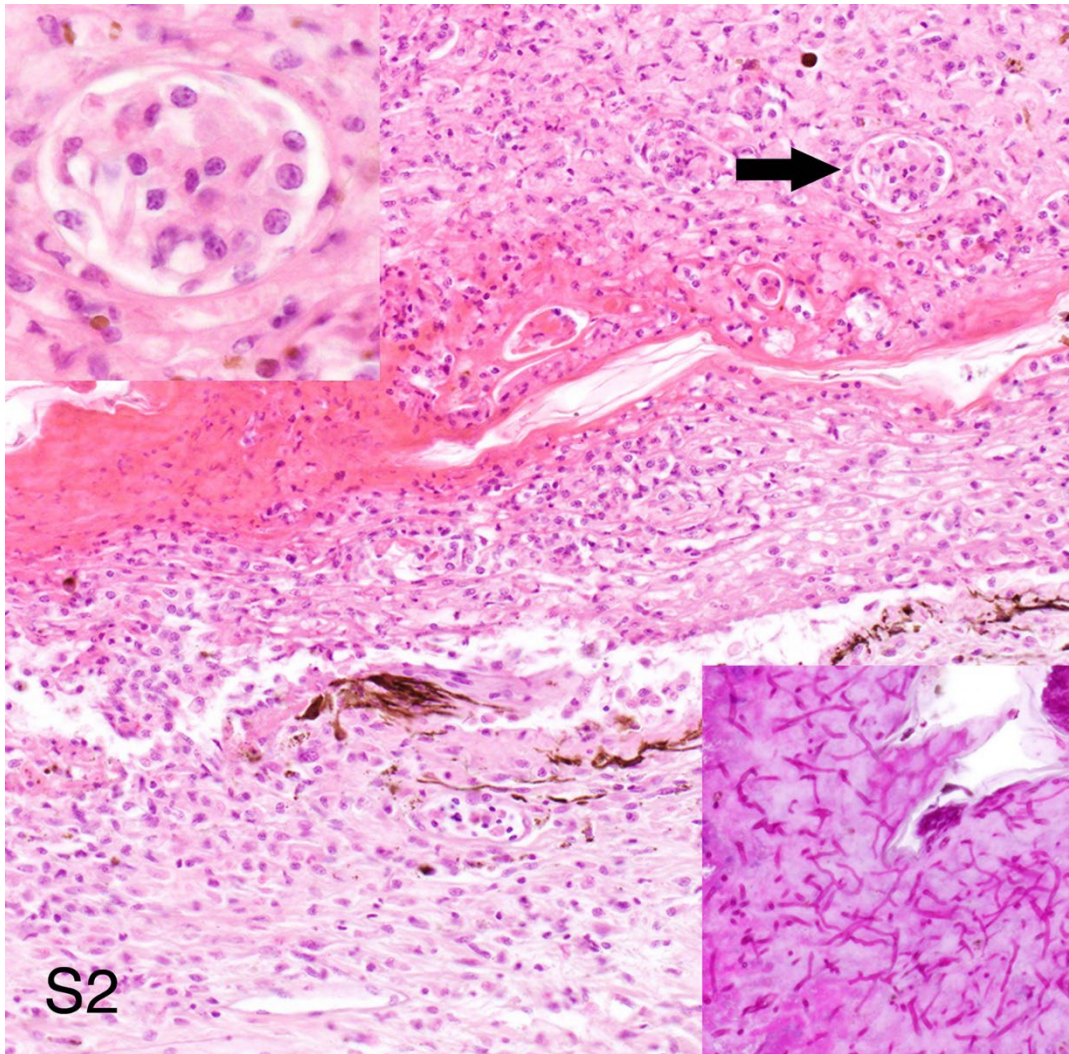
AGAATTGTCGATCTTTGACCAATCATGCCTGACCCCTTTGAACCATGCATTTTTTACCTTGACGCTCTTCAGTAT
ACTAATATGTTTTCCCCCCTTAGGAAGCCGAAGAGTTGGGCAAGAAATCCTTCAAATATGCCTGGGTTCTTGACAA
ATTGAAGG

>Sample_12

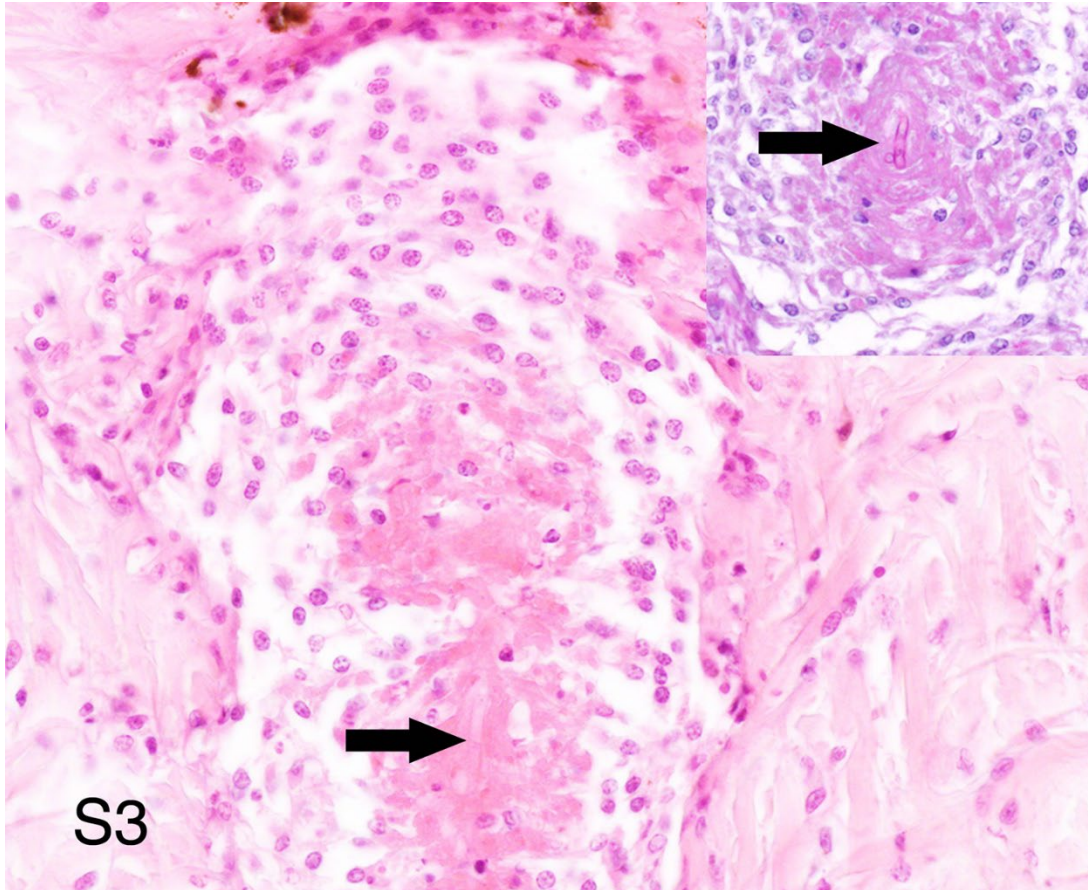
AGAATTGTCGATCTTTGACCAATCATGCCTGACCCCTTTGAACCATGCATTTTTTACCTTGACGCTCTTCAGTAT
GCTAATATGTTTTCACCCCTTAGGAAGCCGAAGAGTTGGGCAAGAAATCCTTCAAATATGCCTGGGTTCTTGACAA
ATTGAAGG



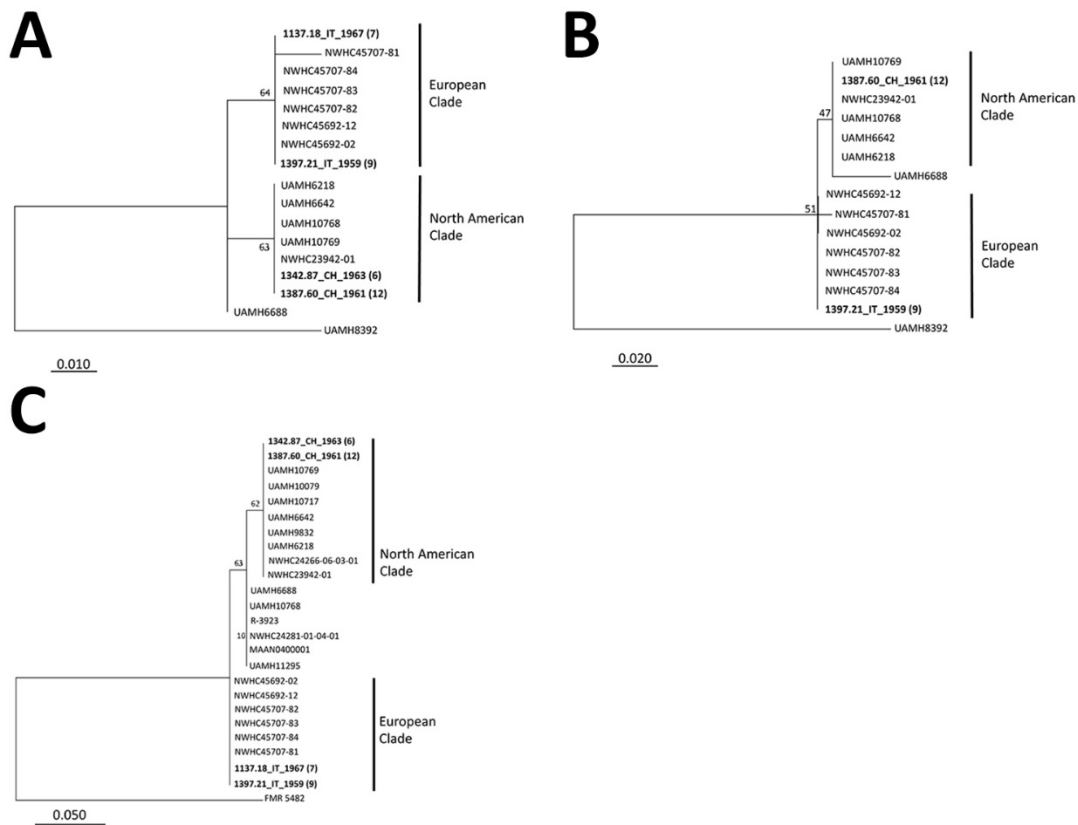
Appendix Figure 1. Skin from *Natrix helvetica* (MHNG1137.18) from study of *Ophiodiomyces ophiodiicola*, etiologic agent of snake fungal disease. The caudal rim of several ventral scales is colored dark tan to brown with variably extensive indentation (ulcerative necrosis, white arrows).



Appendix Figure 2. Skin from *Natrix* sp. from study of *Ophiodiomyces ophiodiicola*, etiologic agent of snake fungal disease. The epidermis is diffusely and severely infiltrated by inflammatory cells. Multifocally, organized cores of histiocytic cells (granulomas) are scattered within the effaced epidermis (black arrow and upper left inset). Numerous fungal elements are highlighted by the Periodic acid Schiff (PAS) stain (lower right inset).



Appendix Figure 3. Skin from *Natrix* sp. from study of *Ophiodiomyces ophiodiicola*, etiologic agent of snake fungal disease. A granuloma embedding a fungal hypha (negative image, black arrow [H&E]; black arrow and inset [PAS]) is expanding within the dermis.



Appendix Figure 4. Phylogenetic analysis of *Ophioidiomyces ophioidicola* clades from North America and Europe, using various PCR primers. Maximum likelihood phylogenetic trees obtained for the A) ACT and B) TEF genes, and C) the 5.8-28s RNA internal transcribed spacer 2. All trees show a clear separation of the clades of *O. ophioidicola* from Europe and North America. Numbers at the nodes show the bootstrap values. The outgroup is the same fungal species for each tree. The *O. ophioidicola*-positive samples identified in this study are listed in bold in the trees. The sample number is shown in brackets. ACT, actin; TEF, transcription elongation factor; ITS, internal transcribed spacer